JOINT CCP4 AND ESF-EACBM NEWSLETTER ON PROTEIN CRYSTALLOGRAPHY

An informal Newsletter associated with the BBSRC Collaborative Computational Project No. 4 on Protein Crystallography and the ESF Network of the European Association of the Crystallography of Biological Macromolecules.

Number 31 June 1995

Contents

Editors: Sue Bailey

The Daresbury Laboratory
Daresbury, Warrington WA4 4AD UK

Keith S. Wilson

EMBL c/o DESY
Notkestrasse 85, D-2000 Hamburg 52
Germany

ON AB INITIO PHASING OF RIBOSOMAL PARTICLES AT VERY LOW RESOLUTION

by

N. Volkmann[1], F. Schlünzen[1], A.G. Urzhumtsev[2,3], E.A. Vernoslova[2,3] A.D. Podjarny[2], M. Roth[4], E. Pebay-Peyroula[4,5], Z. Berkovitch-Yellin[6], A. Zaytzev-Bashan[6] and A. Yonath[1,6]

[1] *Max-Planck Laboratory for Ribosomal Structure, Hamburg, Germany*
[2] *UPR de Biologie Structurale, Parc d'Innovation, Illkirch, C.U. de Strasbourg, France*
[3] *IMPB, RAS, Pushchino, Moscow region, 142292, Russia*
[4] *Institute de Biologie Structurale, Grenoble, France*
[5] *Université Joseph Fourier, Grenoble, France*
[6] *Department of Structural Biology, Weizmann Institute, Rehovot, Israel*

ABSTRACT

Ab initio phasing of ribosomal particles at very low resolution was attempted with several methods based on the amplitude information from native crystals. Some of these methods used simple topological constraints or information about the envelope shape obtained from electron microscopic reconstruction in addition. This paper reviews the approaches used and compares the results obtained for low-resolution X-ray data of the large ribosomal subunit from *Thermus thermophilus* which show a clear agreement in the center-of-mass position as well as in shape information up to a resolution of about 80 Å. Parallel studies on the exploitation of *ab initio* procedures for the localization of heavy atoms at intermediate resolution and their comparison to difference Patterson interpretation are also being performed.

INTRODUCTION

The universal cell organelles facilitating the process of protein biosynthesis are nucleoprotein assemblies called ribosomes. A typical bacterial ribosome has a molecular weight of over 2.3 million and contains 57-73 different proteins and three RNA chains of about 4500 nucleotides arranged in two subunits of unequal size.

Crystals from ribosomes and their complexes with non-ribosomal components as well as from native, chemically modified and mutated ribosomal subunits were obtained [1], diffracting at best to 2.9 Å resolution (for crystals of the large subunits from *Haloarcula marismortui*, [2]). The X-ray data collection is carried out with synchrotron radiation at cryogenic temperatures using flash-frozen crystals [3].

Phasing by multiple isomorphous replacement proved to be extremely complicated and difficult for ribosomal particles, due to lack of isomorphism and to the size of the particles which requires the use of large heavy-atom compounds for derivatization. Nevertheless encouraging preliminary results in that direction were obtained recently [4,5].

Simulation studies and previous experience with derivative data of the large ribosomal subunit of *Bacillus stearothermophilus* indicated that even for a covalently and specifically bound compact heavy-atom compound, the phasing power is negligible at resolutions lower than 50 Å [6,5]. Weighted radially averaged intensity plots show that the scattering behaviour of the large ribosomal subunit is largely dominated by a huge peak around 160 Å resolution which disappears around 50 Å (Figure 1). Weighted intensity plots for the small ribosomal subunit show a similar peak at a resolution of about 100 Å.

These plots indicate the importance of the structure factors at Bragg spacings between infinity and 50 Å for the structure determination of ribosomal particles, especially for cases were only low- to medium-resolution data is available. Since no direct experimental phase information from derivatized crystals is expected in this resolution range, low-resolution studies were initiated.

These studies aim at the determination of accurate low-resolution envelopes which should be valuable for use in phase improvement and extension techniques at higher resolution and for combining electron density information of different crystal forms. *Ab initio* phase information at a resolution substantially higher than 50 Å might also be used for initial phasing of difference maps and the location of heavy-atom sites. Encouraging results were obtained recently, using the following

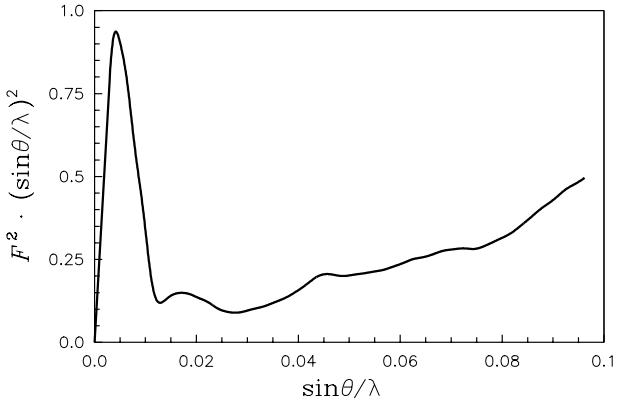

Figure 1: Radially averaged weighted intensity (in arbitrary units) calculated from experimental data from crystals of the large ribosomal subunit of *Haloarcula marismortui*. The main peak is at 160 Å resolution which corresponds to the approximate diameter of the particle. $\sin\theta/\lambda$ is given in $Å^{-1}$.

approaches:

- entropy maximization with log-likelihood gain as a phase set discriminator [7] to determine low-resolution phases [6,8];
- ultralow-resolution (∞-100 Å) R-factor searches at various solvent contrasts to identify the center-of-mass position of the particle [6,9];
- an extension of traditional direct methods [10] to identify the center-of-mass position followed by ellipsoidal modeling applied to X-ray data [11] and neutron data [12];
- application of the few-atom-model method [13] which combines random model generation with clustering techniques to determine a low-resolution envelope [14];
- use of envelopes determined by three-dimensional image reconstruction [15] in low-resolution molecular-replacement studies to determine the position and orientation of the envelope in the unit cell [16];
- application of an approach combining elements of traditional direct methods, envelope refinement, maximum-entropy filtering, likelihood ranking, cross-validation and cluster analysis aiming at phasing at intermediate resolution (likelihood aided positioning and shaping [17]).

All methods listed above were applied to low-resolution X-ray data of the large ribosomal subunit of *Thermus thermophilus*. The data indicate either spacegroup

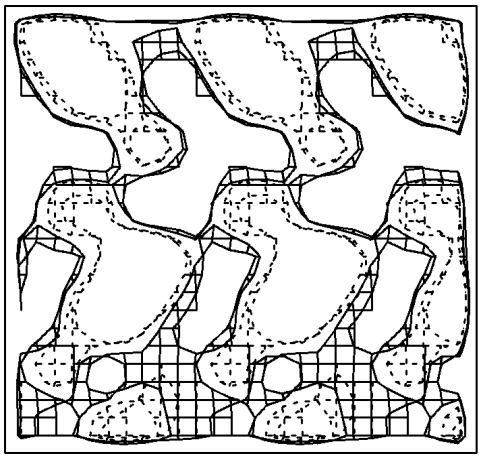

Figure 2: Electron density map at about 80 Å resolution resulting from an application of the maximum-entropy method to a X-ray data set of the large ribosomal subunit of *Thermus thermophilus*. The Figure shows a thin slice in y-direction to demonstrate the crystal contacts. The solid contours are set to the theoretical threshold that should separate particle from solvent. The dashed contours are set as to emphasize the shape of the particle. This shape is very similar to the one obtained by three-dimensional image reconstruction and agrees well with shapes obtained by other methods (see also Table 2 and Figures 5 and 7).

$P4_12_12$ or its enantiomer $P4_32_12$ and a unit cell of $500\pm5 \cdot 500\pm5 \cdot 200\pm5$ $Å^3$. The crystals diffract to a resolution of about 8.7 Å [18]. Spacegroup $P4_12_12$ was assumed for most of the studies presented. There is no evidence to support more than one particle per asymmetric unit and no non-crystallographic symmetry is present within the particle itself.

ENTROPY MAXIMIZATION

In this approach entropy maximization is used as a tool to calculate the saddlepoint approximation of the joint probability distribution of a set of structure factors (basis set) used as constraints in the maximum-entropy equations. The correct phase choice is identified by a log-likelihood gain criterion. This criterion is based on the conditional probability of structure factor amplitudes of a set of reflections that are not used as constraints, given the phase choices and amplitudes for the basis-set reflections.

The application of this method to crystallographic X-ray data from the large ribosomal subunit of *Thermus thermophilus* using the program MICE [19] resulted in a unique solution at about 90-80 Å resolution, identified purely by statistical criteria [8]. Hence, this solution is

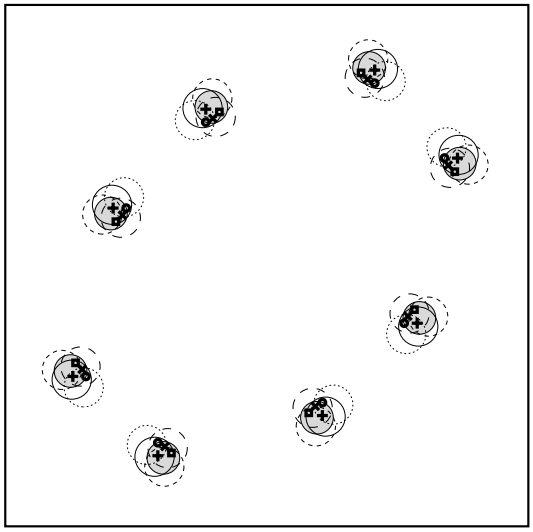

Figure 3: R-factor minima at different solvent densities and positions of the centroids of electron density maps derived by various methods for X-ray data from the large ribosomal subunit of *Thermus thermophilus*. The size of the circles is given by the estimated root-mean-square error of the corresponding position if an estimate was available. The plot is a projection along the z-axis of the whole unit cell. The distance between the positions in the z-direction are of the same order as in the other two directions. GTG denotes goldthioglucose.

based solely on the selection criterion log-likelihood gain and is completely unbiased by any additional assumptions. The resulting map shows features that agree with those of the model obtained by three-dimensional image reconstruction at similar resolution (Figure 2). This result also supports the hypothesis that only one molecule per asymmetric unit is present in the crystal structure.

ULTRALOW-RESOLUTION R-FACTOR SEARCHES

Test calculations using the model obtained by three-dimensional image reconstruction show that the large ribosomal subunit can be well approximated as a single Gaussian sphere of a diameter of 160 Å up to a resolution of 100 Å [6]. Consequently reflections of resolution lower than 100 Å were used for R-factor searches using a Gaussian sphere as a search model. The R-factor minimum theoretically appears at the centroid of the particle electron density, provided a sufficient contrast between the particle and the surrounding solvent density is present.

Searches were performed for four data sets collected from crystals of the large subunit of *Thermus thermophilus* immersed in solutions with different solvent densities using molar amounts of goldthioglucose [9]. An estimate of the root-mean-square error of the positions was achieved by an application of R-factor ratio tests [20] to neighbouring grid points [6]. It was found that the positions of the R-factor minima for all contrasts are in excellent agreement among themselves as well as with the center-of-mass position determined by other methods (Figure 3).

FEW-ATOM MODELS

The low-resolution *ab initio* phasing with few-atom models (FAM) [13] consists of the following steps:

(a) about a million of simple models consisting of a few (usually less than ten) large Gaussian quasi atoms are generated by placing these atoms randomly in the unit cell;

(b) structure factors are calculated for each model from infinity up to a predefined resolution;

(c) the corresponding phase sets are kept if the calculated and observed amplitudes are highly correlated;

(d) a clustering procedure is applied to the surviving phase sets (a few hundred). The procedure generates a tree in which each branching node corresponds to a Fourier synthesis which uses the averaged phases of the contributing members of the cluster. Weights are calculated according to the standard deviation of the phase distributions. The clustering normally yields a small number (2-4) of potential solutions. The correct solution is identified by independent criteria as for example simple packing considerations.

FAM phasing of the large ribosomal subunit of Thermus thermophilus

As a first step, the method was used in its simplest form. The parameters were defined earlier in tests with simple simulated ribosome data [13]. The predefined resolution cutoff was 60 Å. One million models consisting of five Gaussian quasi atoms with a diameter of about 25 Å were generated. 560 models having an amplitude correlation higher than 86% were selected for the cluster analysis.

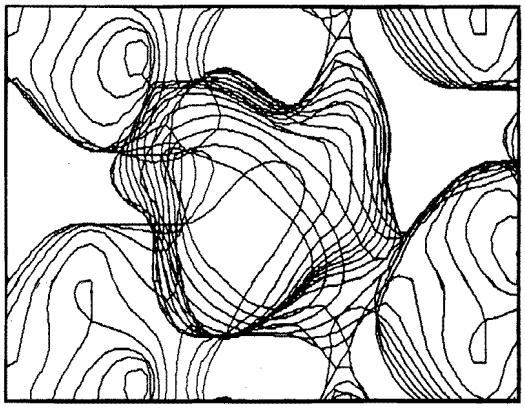

Figure 4: Electron density map at 80 Å resolution derived by an application of the few-atom-model approach to X-ray data from the large ribosomal subunit of *Thermus thermophilus*. This map is in excellent agreement with maps derived by other procedures as well as with the results of low-resolution molecular-replacement studies (see also Table 2 and Figures 5 and 7).

MOLECULAR REPLACEMENT RESULTS

R	N	S	x	y	z	$\mathcal{C}_F$	s
∞	1 (A)	96	0.712	0.107	0.044	95.0	3.7
-90	2 (B)	92	0.284	0.107	0.307	92.8	3.5
	3 (C)	92	0.697	0.119	0.417	89.9	3.1
	4 (D)	96	0.061	0.339	0.289	88.7	3.0
150	1 (A)	96	0.701	0.099	0.039	94.6	3.3
-90	2 (E)	92	0.451	0.348	0.302	91.4	3.1
	3 (B)	92	0.282	0.116	0.307	89.8	3.0
	4 (D)	96	0.074	0.347	0.307	88.7	3.0

Table 1: Amplitude correlation after rigid-body refinement for the most significant molecular-replacement solutions ($s > 3.0$). R denotes resolution in Å, N the peak number, S the spacegroup number and $\mathcal{C}_F$ the amplitude correlation in percent. The signal-to-noise ratio s is given by $(\mathcal{C}_F - \overline{\mathcal{C}_F})/\sigma(\mathcal{C}_F)$, where the mean correlation $\overline{\mathcal{C}_F}$ and its standard deviation $\sigma(\mathcal{C}_F)$ are estimated from a systematic six-dimensional correlation search in a 60 Å^3 box centered at the presumed center of the particle.

The resulting cluster tree was well branched, and incorrect branches at each level were easy to identify by the fact that the electron density was concentrated on the crystallographic dyads. An analysis of the weight distribution as a function of resolution revealed that the final surviving map had an effective resolution of about 110 Å. Although all phases up to 60 Å were used in the clustering procedure, the resulting weights at resolutions higher than 110 Å were consistently very small.

To increase the resolution of the result, a slightly different strategy, applying two criteria simultaneously, was used. The first criterion was the amplitude correlation in the resolution range between 60-120 Å and the second was the phase correlation for reflections between infinity and 120 Å.

The analysis of the corresponding cluster tree resulted in a unique solution which was significantly less noisy than the one described above. There was no density left on the crystallographic dyad and the effective resolution for this synthesis was estimated to be about 80 Å. The resulting electron density map is shown in Figure 4.

MOLECULAR REPLACEMENT

Envelopes determined by electron microscopic three-dimensional image reconstruction [15] were used in low-resolution molecular-replacement studies. During these studies it was assumed that the envelope has the correct chirality although it is not given by the reconstruction technique. Hence, all searches were performed in the two enantiomeric spacegroups $P4_12_12$ (spacegroup number 92) and $P4_32_12$ (96) using the original electron microscopic envelope.

The searches were carried out at the lowest possible resolution to minimize influences of possible disagreements between the electron microscopic envelope model and the actual envelope in the crystal structure. Following [16] the optimal resolution was chosen as follows: 150-90 Å for the rotation search, ∞-90 Å for the translation search and ∞-90 Å or 150-90 Å for the rigid-body refinement step.

Packing considerations were not used during the search procedure. Following the AMoRe strategy [21] only the results after rigid-body refinement were analyzed using the difference in amplitude correlation as the main criterion.

Table 1 shows amplitude correlations of selected solutions for both spacegroups. Peak B was symmetrically related to peak A by an enantiomer transformation. The search result not only indicates the position and the orientation of the envelope but also gives a weak indication for the choice of the spacegroup or the chirality of the envelope. The packing arrangement for peak A was essentially the same as the one obtained by the few-atom-model approach (Figure 5).

DIRECT METHODS AND ELLIPSOIDAL MODELING

This procedure consists of the following steps [10]:

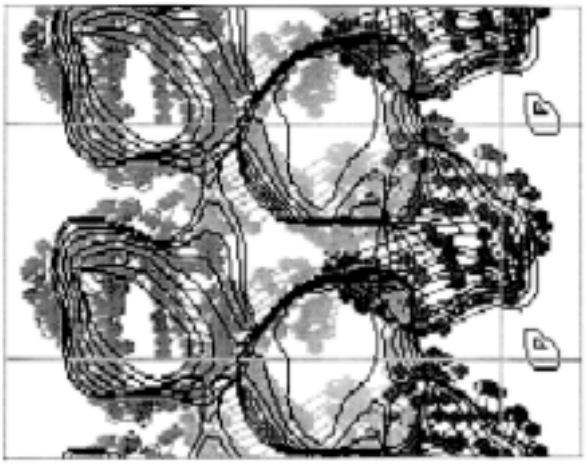

Figure 5: Envelope orientation derived from low-resolution molecular replacement overlaid with an electron density map at 80 Å resolution as derived by an application of the few-atom-model method to low-resolution X-ray data from the large ribosomal subunit of *Thermus thermophilus*.

i. normalization of the observed structure factor amplitudes F by dividing each one by the average of F in a thin resolution shell defined by the miller index of the corresponding reflection;

ii. generation of triplet and quartet phase relationships based on the values of the normalized structure factor amplitudes;

iii. generation of about 100 to 150 phase sets using the MAGEX procedure [22] and subsequent tangent formula refinement of these phase sets. These calculations are performed using the program MITHRIL [23];

iv. for each phase set a map is calculated using the normalized structure factor amplitudes. A peak search is performed and a number of peaks given by the number of molecules in the unit cell are selected according to their height;

v. these coordinates are interpreted as coordinates of point scatterers in the unit cell and structure factors are calculated. These calculated structure factors are compared to the observed normalized structure factors by means of various criteria. The phase set giving the best combined value of these criteria is selected for further treatment;

vi. the phase set is extended in the ultralow-resolution range (∞-120 Å) by addition of calculated phases from the previous step for unphased reflections since MITHRIL only generates phases for the 30 to 35% strongest reflections;

vii. the phases are shifted by π in resolution ranges where the form factor of an ellipsoidal model of the molecule, which is derived by the shape of the Patterson origin peak, is negative.

viii. these phases are subsequently refined and extended by an iterative classical density modification technique, using the non-normalized observed structure factors as amplitudes in the Fourier synthesis.

The method was applied to neutron diffraction data from the large ribosomal subunit of *Haloarcula marismortui* at two different D_2O concentration [12] as well as to X-ray data of the the large ribosomal subunit of *Haloarcula marismortui* and *Thermus thermophilus* [11].

LIKELIHOOD AIDED POSITIONING AND SHAPING

The development of this approach was motivated by some common problems of the procedures described above which became evident during their application to ribosome data:

- only very low-resolution data could be phased (the current limit is at about 80 Å);
- sensitivity to missing or badly measured ultralow-resolution data;
- suboptimal use of available information as for example solvent contrast data or approximate envelopes determined by electron microscopy.

The procedure described here was specifically designed to address these problems for X-ray data from ribosomal particles and will be described elsewhere in detail [17]. Below a brief outline is given (see also Figure 6).

All reflections up to about 30 to 25 Å are used in each step of the calculations to suppress the influence of the ultralow-resolution reflections. The selection of the solution is done solely on the basis of the log-likelihood gain criterion described above in the context of entropy maximization. This ensures an optimal choice in an unbiased Bayesian fashion [24,25].

Optimization of the information contents is ensured by the use of a maximum-entropy filtering step [26], which at the same time gives an estimate for the saddlepoint approximation of the joint probability distribution. This estimate is used to calculate the likelihood [7].

As a tool for combining information agglomerative, hierarchical clustering procedures [27], which is closely related to the one used in the few-atom-model approach,

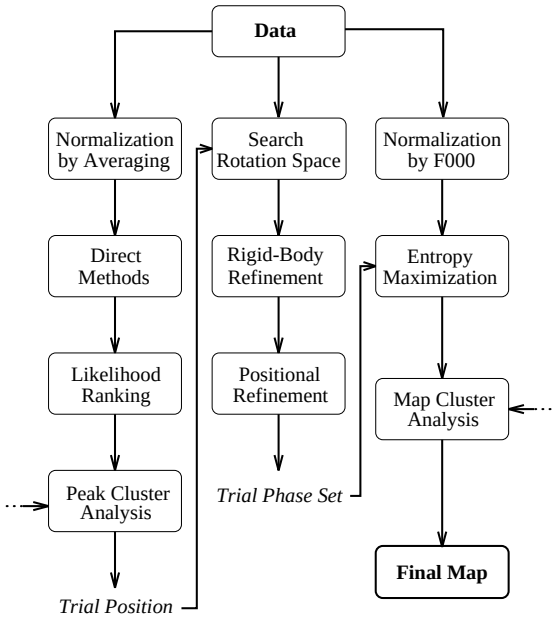

Figure 6: Flow chart of the likelihood aided positioning and shaping procedure. Independent information for cross-validation or improvement of the information content can be entered at the two cluster analysis steps.

are used. Independent information can be easily introduced into the cluster analyses either to cross-validate or to improve the results.

One source of independent information is the application of the same procedure to independent data sets, as from different solvent contrasts or from non-isomorphous crystals, or using the same data set with different envelope approximations. Other sources can be of completely different origin, as for example results of the other procedures described in this paper or multiple isomorphous replacement information. All these sources can be easily combined by clustering.

The actual procedure employed consists of two distinct parts. The first is to establish the center-of-mass position of the particle inside the unit cell, the second consists of introducing shape information.

Standard direct methods are applied, treating the data as approximating a single point scatterer and normalizing accordingly. The log-likelihood gain criterion is calculated via the saddlepoint approximation using the program MICE and is used as a phase set discriminator.

The center-of-mass position is found by grouping the maps with high likelihood gain signals by a cluster analysis of peak positions using only the highest peak in each map. Outliers are easily identified by their large distances from the main cluster and are eliminated. The center of the remaining cluster gives an estimate of the center-of-mass position and the scattering of the contributing peaks around the center gives an estimate of the root-mean-square error of that position.

Knowing the position of the molecule, shape information can be introduced using approximate envelopes. Envelope models of the large ribosomal subunit have a nominal resolution of about 27 Å [15] and are represented by about 1700 Gaussian scatterers distributed uniformly within the envelope. This representation is used in an exhaustive search of rotation space at the predetermined position. For each orientation the scatterer positions are refined against the observed amplitudes by rigid-body and subsequent individual positional refinement. Phase sets are calculated for each refined set of scatterers. These phase sets are subjected to entropy maximization to suppress bias and noise which might have been introduced by the use and refinement of the Gaussian scatterers. The log-likelihood gain is calculated via the saddlepoint approximation for each set.

The final step of the procedure consists of a cluster analysis based on the correlation between the resulting electron densities. A consistent cluster of maps associated with high likelihood gain signals is located by varying resolution and likelihood cutoffs. After location, the likelihood cutoff is chosen as to maximize the correlation between the maps in the cluster over the complete resolution range. Then all maps in the cluster are merged in reciprocal space and weights are calculated from the actual phase distributions within the cluster interpreting them as an experimental draw from a von Mise distribution [28].

The method generates phase sets with reasonable completeness and weight distributions up to a resolution of about 30 to 40 Å (Figure 8). The maximum resolution achievable is mainly limited by the quality and resolution of the envelope approximations used and should be considerably higher if higher resolution envelope information were available.

The procedure was applied to native X-ray data of the large subunit of *Thermus thermophilus* using two different envelope approximations and to a X-ray solvent contrast series of the large subunit of *Haloarcula marismortui*. This work will be described elsewhere [29].

Phases and weights between 70 and 30 Å resolution obtained for the *Haloarcula marismortui* data were used to locate heavy-atom sites by means of a difference Fourier calculations. The same sites were found independently by difference Patterson interpretation [4]. Furthermore the overall shape and the internal distribution of electron density at a resolution of about 40 Å obtained for the large ribosomal subunits of *Thermus thermophilus*

CORRELATION TABLE

	FAM	DM	LAPS	SP
ME	96.6	89.2	95.8	56.1
FAM	–	92.3	98.0	57.2
DM	–	–	93.1	61.9
LAPS	–	–	–	54.2

Table 2: Correlation coefficients C_ϕ (Equation 1) between phase sets obtained by various methods for X-ray data of the large ribosomal subunit of *Thermus thermophilus*. Resolution cutoff was set to 80 Å, C_ϕ is given in percent.

ME:	Maximum entropy
FAM:	Few-atom models
DM:	Direct methods and ellipsoidal modeling
LAPS:	Likelihood aided positioning and shaping
SP:	Sphere at the R-factor minimum

and *Haloarcula marismortui* by this method agree well and the agreement of preliminary low-resolution solvent flattened maps derived by multiple isomorphous replacement and maps derived by this method for the large ribosomal subunit of *Haloarcula marismortui* and the small subunit of *Thermus thermophilus* is striking [4,17].

COMPARISON OF RESULTS

All methods described above were applied to low-resolution X-ray data of the large ribosomal subunit of *Thermus thermophilus*. Figure 3 shows the coincidence of the center-of-mass position as calculated by these procedures.

As a criterion for the similarity of the derived phase sets the following correlation function in reciprocal space was chosen:

$$C_\phi = \frac{\sum w_1 F_1 \; w_2 F_2 \cos(\phi_1 - \phi_2)}{(\sum (w_1 F_1)^2 \sum (w_2 F_2)^2)^{1/2}} \qquad (1)$$

F_i is the structure factor amplitude, w_i and ϕ_i are the weight and the phase calculated by phasing method i. The summation extends over all reflections for which both weights w_i are greater than 0.1.

This function is closely related to the real-space electron density correlation coefficient [30] but is not identical to it since reflections with weights less than 0.1 are omitted from the summation. C_ϕ gives a notion of how well the phase indications of the methods agree for reflections that are estimated as reasonably well phased for

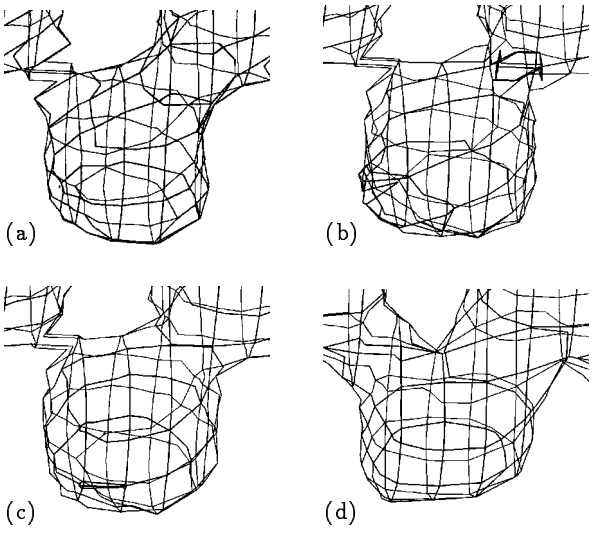

Figure 7: Electron density maps at about 80 Å resolution obtained for X-ray data of the large ribosomal subunit of *Thermus thermophilus*. (a) is derived by likelihood aided positioning and shaping, (b) by entropy maximization, (c) by the few-atom-model approach and (d) by direct methods followed by ellipsoidal modeling.

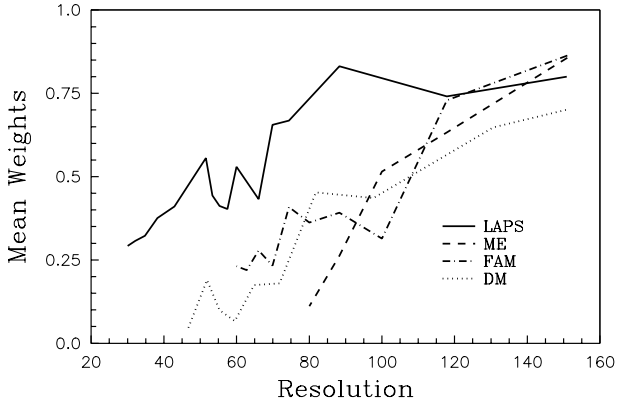

Figure 8: Mean weights calculated for various methods applied to X-ray data of the large ribosomal subunit of *Thermus thermophilus*. Resolution is given in Å. The weights for FAM and LAPS are calculated from the phase distribution within the final cluster. The weights of ME are directly related to the likelihood of the corresponding phase choice to be correct [19]. The weights for DM are calculated according to the assumption that the estimated phase error of reflections phased by MITHRIL averages at about 45° over the whole resolution range. Phases calculated from the peak position were assumed to have an average error of about 60°. A weight of zero was assigned to all unphased reflections for all procedures.

both methods compared. The results of the calculations are shown in Table 2.

Entropy maximization, the few-atom-model method and likelihood aided positioning and shaping gave essentially the same phase indications at a resolution of about 80 Å. This is also supported by the small differences seen in a visual inspection of the corresponding electron density maps (Figure 7). The direct method approach gives a slightly lower correlation C_ϕ with each of these methods but performs clearly better than a simple sphere at the center-of-mass position (Table 2).

Figure 8 shows the mean weight distributions as a function of resolution for the procedures mentioned. These curves give an indication of the phasing power as a function of resolution and an estimate of the effective resolution of the resulting electron density maps.

ACKNOWLEDGMENTS

We give our sincere thanks to all members of the Max-Planck Laboratory for Ribosome Structure in Hamburg and of the Max-Planck Institute for Molecular Genetics in Berlin, Germany as well as to all members of the ribosome group of the Department of Structural Biology, Weizmann Institute, Rehovot, Israel for kindly supplying experimental data for these studies and for illuminating discussions. We thank Dr. W.S. Bennett for critically reading the manuscript.

N.V. would like to thank Drs. C.J. Gilmore and C. Carter for making available their respective versions of MICE and Dr. G. Bricogne for many stimulating discussions in entropy matters.

A.U., E.V. and A.P. thank Dr. D. Moras for continuing support and Dr. B. Rees for useful discussions. The FAM programs have been developed within a collaboration with Dr. V. Lunin and his laboratory (IMPB, Pushchino) financed by the CNRS-RAS cooperation agreement. A.U., E.V. and A.P. have been supported by the CNRS through the UPR 9004, by the Institut de la Santé et de la Recherch Médicale and by the Centre Hospitalier Universitaire Régionale.

The collaboration between the Grenoble and the Hamburg groups was supported by the DAAD-PROCOPE foundation, and that between the Grenoble and the Israeli group by AFIRST, the Israel-France Ministries of Science and Technology program.

REFERENCES

[1] Z. Berkovitch-Yellin, W.S. Bennett, A. Yonath (1992), CRC Rev. Biochem. & Mol. Biol., **27**, 403.

[2] K. von Böhlen, I. Makowski, H.A.S. Hansen, H. Bartels, A. Zaytzev-Bashan, S. Meyer, C. Paulke, F. Franceschi, A. Yonath (1991), J. Mol. Biol. **222**, 11.

[3] Z. Berkovitch-Yellin, H.A.S. Hansen, S. Weinstein, M. Eisenstein, K. von Böhlen, I. Agmon, U. Evers, J. Thygesen, N. Volkmann, H. Bartels, F. Schlünzen, A. Zaytzev-Bashan, R. Sharon, I. Levin, A. Dribin, G. Kryger, W.S. Bennett, F. Franceschi, A. Yonath (1993), in: 'Synchrotron Radiation in Biosciences', (Ed.: B. Chance *et al.*), Clarendon Press, pp 61-70.

[4] F. Schlünzen, H.A.S. Hansen, J. Thygesen, W.S. Bennett, N. Volkmann, I. Levin, J. Harms, H. Bartels, A. Bashan, Z. Berkovitch-Yellin, I. Sagi, F. Franceschi, S. Krumbholz, M. Malemud, S. Weinstein, I. Agmon, N. Böddeker, S. Morlang, R. Sharon, A. Dribin, E. Maltz, M. Peretz, V. Weinrich, A. Yonath (1995), Biochemistry and Cell Biology, in Press.

[5] H. Bartels, W.S. Bennett, H.A.S. Hansen, M. Eisenstein, S. Weinstein, J. Müssig, N. Volkmann, F. Schlünzen, I. Agmon, F. Franceschi, A. Yonath (1995), J. Peptide Sciences, in Press.

[6] N. Volkmann (1993), 'Maximum Entropie und das Phasenproblem für ribosomale Kristalle', *Ph.D. Thesis*, University of Hamburg, Germany.

[7] G. Bricogne (1984), Acta Cryst. **A40**, 410.

[8] N. Volkmann (1995), in: 'Entropy, Likelihood, Baysian Inference and their Application in Crystal Structure Determination', (Ed.: G. Bricogne), American Crystallographic Association, in Press.

[9] F. Schlünzen (1994), 'Kristallographische Untersuchungen der 50S ribosomalen Untereinheit von *Thermus thermophilus*', *Ph.D. Thesis*, University of Hamburg, Germany.

[10] M. Roth, E. Pebay-Peyroula (1995), in: 'Entropy, Likelihood, Baysian Inference and their Application in Crystal Structure Determination', (Ed.: G. Bricogne), American Crystallographic Association, in Press.

[11] A. Zaytzev-Bashan (1995), 'Crystallographic Studies on the Large Ribosomal Subunit from Halophilic and Thermophilic Bacteria', *Ph.D. Thesis*, Weizmann Institute, Rehovot, Israel.

[12] M. Roth, E. Pebay-Peyroula, Personal Communication.

[13] V.Yu. Lunin, N.L. Lunina, T.E. Petrova, E.A. Vernoslova, A.G. Urzhumtsev, A.D. Podjarny (1995), Acta Cryst. **D51**, in Press.

[14] A. Urzhumtsev, E.A. Vernoslova, A.D. Podjarny, Personal Communication.

[15] A. Yonath, K.R. Leonard, H.G. Wittmann (1987), Science **236**, 813.

[16] A.G. Urzhumtsev, A.D. Podjarny (1995), Acta Cryst. **D51**, in Press.

[17] N. Volkmann, Manuscript in Preparation.

[18] N. Volkmann, S. Hottenträger, H.A.S. Hansen, A. Zaytzev-Bashan, R. Sharon, A. Yonath, H.G. Wittmann (1990), J. Mol. Biol. **216**, 239.

[19] G. Bricogne, C.J. Gilmore (1990), Acta Cryst. **A46**, 284.

[20] W.C. Hamilton (1965), Acta Cryst. **18**, 502.

[21] J. Navaza (1994), Acta Cryst. **A50**, 157.

[22] S.E. Hull, D. Viterbo, M.M. Woolfson (1981), Acta Cryst. **A37**, 566.

[23] C.J. Gilmore (1984), J. Appl. Cryst. **17**, 42.

[24] J. Neyman, E. Pearson (1933), Philos. Trans. R. Soc. London Ser. **A231**, 289.

[25] G. Bricogne (1988), Acta Cryst. **A44**, 517.

[26] S.F. Gull, G.J. Daniell (1978), Nature, **272**, 686.

[27] R.R. Sokal, P.H.A. Sneath (1963), 'Principles of Numerical Taxonomy', W.H. Freeman, San Francisco.

[28] R. von Mise (1918), Physik. Zeitschr. **XIX**, 490.

[29] N. Volkmann, H.A.S. Hansen, F. Schlünzen, A. Zaytzev-Bashan, A. Yonath, Manuscript in Preparation.

[30] V.Yu. Lunin, M.M. Woolfson (1993), Acta Cryst. **D49**, 530.